

# Overturning circulation driven by breaking internal waves in the deep ocean

Maxim Nikurashin<sup>1,2</sup> and Raffaele Ferrari<sup>3</sup>

Received 25 March 2013; revised 5 May 2013; accepted 6 May 2013; published 21 June 2013.

[1] A global estimate of the water-mass transformation by internal wave-driven mixing in the deep ocean is presented. The estimate is based on the energy conversion from tidal and geostrophic motions into internal waves combined with a turbulent mixing parameterization. We show that internal wave-driven mixing in the deep ocean can sustain 20–30 Sv of water-mass transformation. One third or more of this transformation is attributed to lee waves generated by geostrophic motions flowing over rough topography, primarily in the Southern Ocean. While these results are uncertain due to many assumptions, poorly constrained parameters and data noise that enter in the calculation, the result that lee wave-driven mixing plays an important role in the abyssal ocean circulation is likely robust. The implication is that lee wave-driven mixing should be represented in ocean and climate models, but currently it is not. **Citation:** Nikurashin, M., and R. Ferrari (2013), Overturning circulation driven by breaking internal waves in the deep ocean, *Geophys. Res. Lett.*, 40, 3133–3137, doi:10.1002/grl.50542.

## 1. Introduction

[2] The zonally averaged overturning circulation of the ocean is composed of two shallow wind-driven cells, confined to the upper kilometer on both sides of the equator, and two interhemispheric deep cells stacked on top of each other that span the rest of the oceans [e.g., Pedlosky, 1996; Marshall and Speer, 2012, review]. The wind-driven cells flow mostly along density surfaces in the ocean interior, and all water-mass transformations are confined to the surface. The deep cells sink to the abyss in the North Atlantic and around the Antarctic continent, where heat and freshwater loss transforms light surface waters to dense deep waters. The dense waters must somehow come back to the surface to complete the overturning loop and return to the sinking regions as light waters. The upward pathway of these waters and the underlying physical mechanisms remain poorly understood. It is believed that the return flow of the mid-depth cell, formed in the North Atlantic, is primarily along density surfaces all the way to the Southern Ocean, where the dense waters come to the surface and are transformed back to light

waters [e.g., Marshall and Speer, 2012, review]. In contrast, the abyssal waters, formed around Antarctica, are believed to upwell from the abyss to mid-depth across density surfaces, and thus the transformation into lighter waters occurs in the ocean interior through mixing with overlying water masses [Stommel, 1958; Munk, 1966; Nikurashin and Vallis, 2011].

[3] Oceanic motions at scales larger than tens of kilometers flow along density surfaces and cannot drive water-mass transformations [e.g., Pedlosky, 1996]. Such transformations can instead be sustained by mixing across density surfaces generated by small-scale turbulent motions. While mixing processes remain poorly understood and direct mixing observations are sparse in the ocean, available fine- and micro-structure measurements suggest that breaking internal waves on scales of less than 10 m are a primary source of small-scale turbulent mixing in the ocean interior [Polzin et al., 1997; Gregg, 1989]. In most of the ocean, mixing rates are an order of magnitude too weak to sustain the observed overturning circulation [e.g., Ledwell et al., 1998]. However, internal gravity wave breaking and mixing are strongly enhanced above rough topography [e.g., Polzin et al., 1997; Naveira Garabato et al., 2004]. Theoretical and numerical studies suggest that internal waves are efficiently generated by deep tidal [e.g., Garrett and Kunze, 2007, review] and geostrophic motions [Nikurashin and Ferrari, 2010a; Nikurashin and Ferrari, 2010b] flowing over rough small-scale topography. These waves then radiate into the ocean interior, interact nonlinearly, and transfer energy to smaller scale waves. At scales of less than 10 m, the waves become unstable and overturn resulting into bursts of mixing [e.g., Polzin, 2004; Nikurashin and Legg, 2011].

[4] In addition to breaking internal waves, there are other sources of mixing in the ocean, such as bottom boundary layer turbulence, hydraulic jumps, loss of balance by meso-scale eddies, entrainment into the deep water plumes, and geothermal heating. However, the contribution of these sources of mixing to the global water-mass transformation remains uncertain. Observations suggest that mixing in the stratified ocean interior is primarily sustained by breaking internal gravity waves [e.g., Garrett and St. Laurent, 2002, review]. This mixing is the focus of our paper; we estimate the rate of abyssal water-mass transformation (and hence, the rate of the overturning circulation) associated with breaking internal waves generated by tidal and geostrophic motions flowing over rough topography.

## 2. Method

[5] We use previous estimates of the energy conversion into internal waves by tides [Nycander, 2005] and geostrophic motions [Nikurashin and Ferrari, 2011] and a recent parameterization [St. Laurent et al., 2002] to estimate the rate

Additional supporting information may be found in the online version of this article.

<sup>1</sup>Institute for Marine and Antarctic Studies, University of Tasmania, Hobart, Australia.

<sup>2</sup>ARC Center of Excellence for Climate System Studies, Australia.

<sup>3</sup>Department of Earth, Atmospheric and Planetary Sciences, Massachusetts Institute of Technology, Cambridge, MA, USA.

Corresponding author: M. Nikurashin, Institute for Marine and Antarctic Studies, University of Tasmania, Hobart, Australia. (man@alum.mit.edu)

©2013. American Geophysical Union. All Rights Reserved.  
0094-8276/13/10.1002/grl.50542

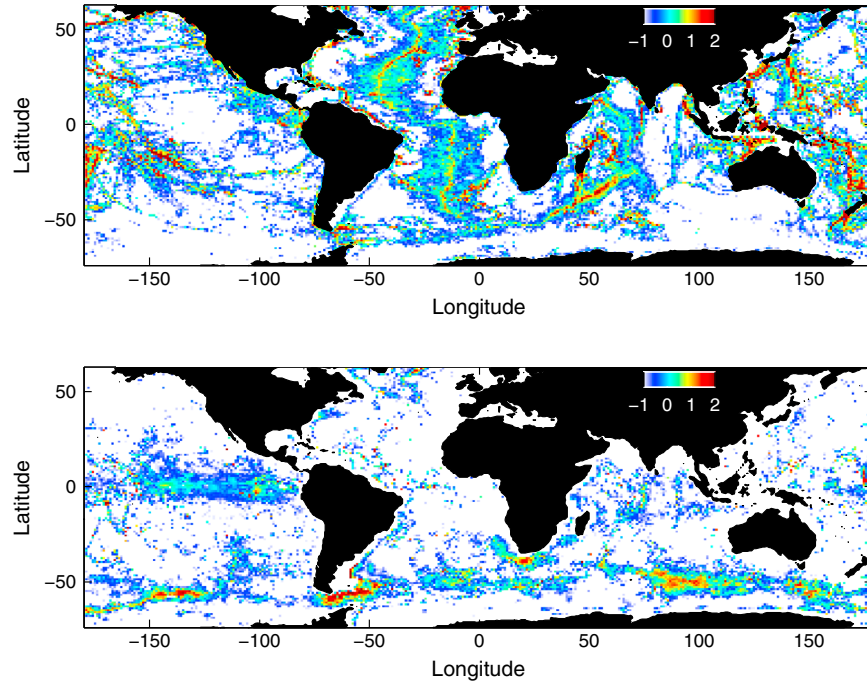


**Figure 1.** Global distribution of the energy conversion in  $[\log_{10}(\text{mW m}^{-2})]$  from (upper panel)  $M_2$  barotropic tide and (lower panel) geostrophic motions into internal tides and lee waves, respectively.

of mixing generated by these waves. Then, we apply the water-mass transformation framework [Walín, 1982] to convert mixing into water-mass transformation rates.

## 2.1. Wave Radiation Estimate

[6] Stratified tidal and geostrophic currents flowing over rough bottom topography generate internal tides and lee waves, respectively. In the limit of small topographic steepness, i.e. when the topographic slope is smaller than the internal wave slope, the wave generation problem can be solved analytically for an arbitrary bottom topography. Resulting linear theory expressions for the energy conversion from tidal and geostrophic flows are summarized in the supplementary material. These expressions are applied to stratification obtained from ocean hydrographic data, bottom velocity obtained from global tidal and ocean models, and topography obtained from satellite altimetry and ship single-beam echo soundings to estimate the global distributions of the energy conversion into internal waves. The reader is referred to Nycander [2005] and Nikurashin and Ferrari [2011] for a more detailed presentation of the wave radiation estimates. Here we simply use these previous estimates.

[7] Global estimates of the energy conversion into internal tides [Nycander, 2005] (internal waves generated by barotropic tides), and lee waves [Nikurashin and Ferrari, 2011] (internal waves generated by geostrophic motions) are shown in Figure 1. Tidal energy conversion takes place in all ocean basins, because of the global extent of tidal motions and is enhanced along mid-ocean ridges and major topographic features. The globally integrated energy conversion from tidal motions into internal tides in the deep ocean is about 1 TW ( $1 \text{ TW} = 10^{12} \text{ W}$ ), which is comparable to the total power input into the large-scale ocean circulation from atmospheric winds [Wunsch, 1998].

In contrast, lee waves are generated primarily in the Southern Ocean, where deep geostrophic flows are strongest and topography is rough on scales shorter than  $O(10 \text{ km})$ . The globally integrated energy conversion from geostrophic motions into lee waves is 0.2 TW, weaker than that from tides. A similar global estimate by Scott *et al.* [2011] reports slightly higher global energy conversion into lee waves, up to 0.4 TW. The energy conversion into lee waves, however, dominates over that into internal tides in the Southern Ocean, where tidal motions are generally weak. In the Southern Ocean, lee wave generation is enhanced in regions of strong currents and high eddy activity such as the Drake Passage and the lee of the Kerguelen Plateau.

## 2.2. Ocean Stratification

[8] The ocean density distribution is taken from the World Ocean Circulation Experiment hydrographic atlas [Gouretski and Koltermann, 2004]. The zonally averaged density distribution and its vertical derivative, the stratification, are plotted in the upper panel of Figure 2. The stratification is largest in the upper kilometer of the ocean (i.e., in the thermoclines maintained by the wind-driven overturning cells) and is small, but not negligible, below it. Density contours at mid-depth correspond to the upper interhemispheric cell of the overturning circulation and outcrop both in the North Atlantic and in the Southern Ocean, while density contours in the abyssal ocean outcrop only in the Southern Ocean and correspond to the lower cell of the overturning circulation. The lower cell starts through convection of dense waters around Antarctica, flows north at the bottom of all ocean basins, becomes progressively lighter as it is being mixed with lighter waters, and finally comes back south to come to the surface in the Southern Ocean.

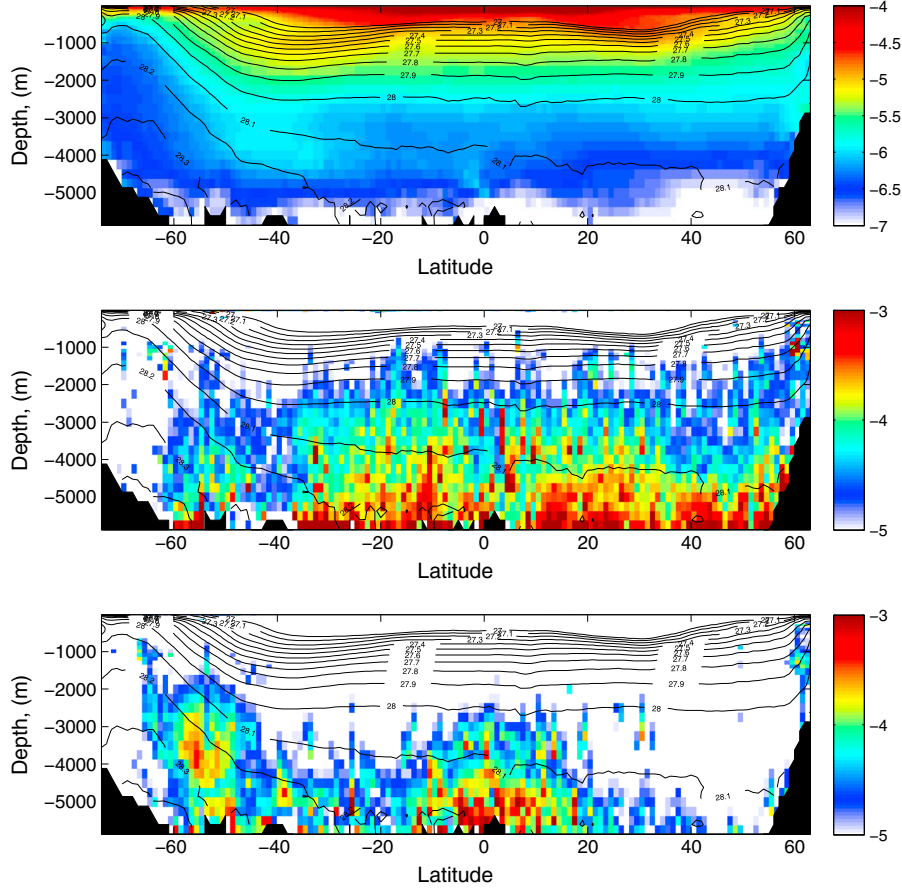


**Figure 2.** Global zonally averaged sections of (upper panel) stratification frequency  $N^2$  in  $[\log_{10}(\text{s}^{-2})]$ , (middle panel) diapycnal mixing  $\kappa_v$  from internal tides in  $[\log_{10}(\text{m}^2 \text{s}^{-1})]$ , and (lower panel) diapycnal mixing  $\kappa_v$  from lee waves in  $[\log_{10}(\text{m}^2 \text{s}^{-1})]$ . Black contours are isoline of neutral density  $\gamma_n$  in  $[\text{kg m}^{-3}]$ . Region shaded in black is the zonally averaged topography.

### 2.3. Mixing Parameterization

[9] We now attempt to quantify how the energy radiated in tidal and lee waves is transferred down to small scales, where breaking and mixing occur. *St. Laurent et al.* [2002] proposed a semi-empirical parameterization that expresses the strength and vertical profile of mixing associated with the topographic radiation of internal waves in the ocean. This parameterization expresses the turbulent kinetic energy dissipation rate  $\epsilon$  as a function of the energy  $E(x,y)$  radiated into internal waves from the ocean bottom as a function of longitude  $x$  and latitude  $y$ ,

$$\epsilon(x,y,z) = qE(x,y)F(z), \quad (1)$$

where  $q$  is the fraction of radiated energy going locally into dissipation, taken to be 30%.  $F(z)$  is the empirical vertical redistribution function, representing the rate at which waves break as a function of height above bottom  $z$ , given by

$$F(z) = \frac{e^{-(H+z)/\zeta}}{\zeta(1 - e^{-H/\zeta})}, \quad (2)$$

where  $H$  is the total depth of the water column and  $\zeta$  is the vertical decay scale of turbulence taken to be 500 m. In the supplementary material, we explore a wide range of values of  $q$  and  $\zeta$ .

[10] The turbulent energy dissipation  $\epsilon$  is related to the effective diffusivity  $\kappa_v$  [Osborn, 1980], which measures the rate at which a patch of tracer ( $\text{CO}_2$ , heat, ...) spreads as a function of time, as follows

$$\kappa_v = \Gamma \frac{\epsilon}{N^2}, \quad (3)$$

where  $\Gamma$  is the mixing efficiency, i.e. the fraction of the turbulent dissipation rate  $\epsilon$  that goes into raising the potential energy, taken to be 0.2 and  $N$  is the stratification frequency.

### 2.4. Water-mass Transformation

[11] The volume  $V$  between a neutral density surface  $\gamma_n^*$  and the bottom of the ocean changes either through the water-mass transformation by air-sea heat and freshwater fluxes at the surface or through the water-mass transformation by diapycnal mixing in the ocean interior,

$$\frac{\partial V}{\partial t} = -S + D, \quad (4)$$

where  $S$  is the surface-integrated water-mass transformation by the air-sea fluxes, and  $D$  is the volume-integrated water-mass transformation by interior mixing. In equilibrium, the transformation by surface fluxes must be balanced by the transformation by interior mixing, i.e.  $S=D$ . Following

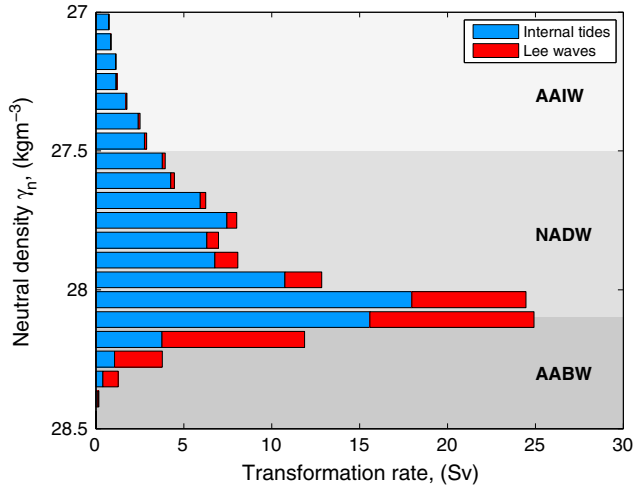


**Figure 3.** A stacked bar diagram of the water-mass transformation rates in [Sv] ( $1 \text{ Sv} = 10^6 \text{ m}^3 \text{ s}^{-1}$ ) by (blue) internal tide-driven diapycnal mixing and (red) lee wave-driven diapycnal mixing as a function of neutral density  $\gamma_n$ .

the commonly used water-mass transformation framework [Walín, 1982], we estimate the interior transformation  $D$  as

$$D(\gamma_n^*) = -\frac{\partial}{\partial \gamma_n^*} \int_{\gamma_n > \gamma_n^*} \frac{\partial}{\partial z} (\kappa_v N^2) dV. \quad (5)$$

Note, that we consider here only mixing processes due to breaking of internal gravity waves and thus do not account for water-mass transformation by processes due to the nonlinear equation of state such as thermobaricity and cabelling [e.g., Klocker and McDougall, 2010].

### 3. Results

[12] We obtain a global three-dimensional distribution of internal wave-driven mixing in the ocean by applying the *St. Laurent et al.* [2002] parameterization to stratification and energy conversion estimates. The zonally averaged internal tide and lee wave-driven mixing is shown in the middle and lower panels in Figure 2 to illustrate the global distribution of mixing with depth. Consistent with observations, the diapycnal diffusivities are fairly constant in the ocean interior of  $O(10^{-5}) \text{ m}^2 \text{ s}^{-1}$  [e.g., Ledwell et al., 1998] and enhanced within a kilometer of rough topography [e.g., Polzin et al., 1997; Naveira Garabato et al., 2004]. The internal tide-driven mixing is concentrated in the bottom kilometer of the ocean and widespread across all latitudes. The diapycnal diffusivities vary generally from  $O(10^{-3}) \text{ m}^2 \text{ s}^{-1}$  near the bottom to background values within a kilometer from the bottom. Only in the Southern Ocean radiation of internal tides and the associated mixing are weak.

[13] Zonally averaged lee wave-driven mixing is enhanced in the equatorial region and in the Southern Ocean, where the associated energy conversion is large in Figure 1. The diapycnal diffusivities are comparable in the two regions, even though the energy conversion is weaker in the equatorial region, because it takes less energy to mix the weakly stratified equatorial bottom waters than the more heavily stratified Southern Ocean waters (the diapycnal diffusivity is inversely proportional to stratification). Also, the strongest mixing of  $O(10^{-3}) \text{ m}^2 \text{ s}^{-1}$  appears to take place a few

kilometers above bottom in the Southern Ocean, because the highest conversion rates are found in the Drake Passage, where the ocean depth is a few kilometers shallower than in the Southern Ocean abyssal plains. Overall, most of the tidal and lee wave-driven mixing takes place on neutral density surfaces greater than  $28 \text{ kg m}^{-3}$ , i.e. in the Antarctic Bottom Water (AABW) formed around the Antarctic continent.

[14] Turbulent mixing across density surfaces results in the transformation of water masses, i.e. in a water-mass flux across density surfaces. In Figure 3, we show estimates of the water-mass transformation associated with internal wave-driven mixing as a function of neutral density. We find that internal wave-driven mixing in the ocean interior sustains up to 25 Sv of water-mass transformation across the  $28\text{--}28.2 \text{ kg m}^{-3}$  density surfaces. This maximum value is comparable to the peak water-mass transformation rates inferred for these dense water masses from surface air-sea fluxes [Speer and Tziperman, 1992; Marshall et al., 1999; Nurser et al., 1999] and inverse box models [e.g., Lumpkin and Speer, 2007]. The density surfaces where the water-mass transformation is largest correspond roughly to the boundary between the upper and lower cells of the meridional overturning circulation, associated with the North Atlantic Deep Water (NADW) and AABW masses. The density range of this maximum is set by the distribution of water masses with respect to topography in the ocean, rather than by the vertical profile of mixing. The largest mixing is confined very near the bottom topography, because mixing decays exponentially with height above bottom. Hence the water-mass transformation driven by mixing tracks closely the ocean bottom topography. For the present climate, this distribution is such that the mixing impact is largest at the boundary between AABW and NADW.

[15] The water-mass transformation above  $28 \text{ kg m}^{-3}$  is dominated by internal tide-driven mixing and varies from 1–3 Sv in the upper ocean on density surfaces corresponding to the Antarctic Intermediate Water to 15–20 Sv at mid-depth on density surfaces corresponding to NADW and AABW. The mixing-driven transformation of 1–3 Sv in the upper ocean is smaller than the transformation by surface fluxes [Speer and Tziperman, 1992; Marshall et al., 1999; Nurser et al., 1999]. This is consistent with the present notion that mixing drives a small fraction of transport in the upper ocean, but accounts for most transport in the abyss [e.g., Marshall and Speer, 2012, review]. In terms of equation (4), the upper cell experiences surface buoyancy gain in the south and surface buoyancy loss in the north, so that  $S$  and  $D$  are small residuals. In the lower cell, the surface buoyancy loss around Antarctica is balanced by interior mixing  $D$ . The water-mass transformation by lee wave-driven mixing reaches up to 5–10 Sv and is limited to the NADW and AABW masses, as it hardly extends above the  $28 \text{ kg m}^{-3}$  density surface. Lee wave-driven mixing has a comparable impact, in terms of the global water-mass transformation rate, as internal tide-driven mixing, even though lee wave generation is weaker and limited to the Southern Ocean.

### 4. Summary and Discussion

[16] The main result of this work is that internal wave-driven mixing drives up to 25 Sv of waters from the abyss towards the surface. This transport peaks at the  $28\text{--}28.2 \text{ kg m}^{-3}$

density surfaces, corresponding to the interface between the NADW and AABW masses [Lumpkin and Speer, 2007]. There are three other unique and important results. First, lee waves generated by geostrophic eddies flowing over rough topography drive most of the mixing in the Southern Ocean and account for one third or more of the global water-mass transformation. Second, the distribution of the internal wave-driven water-mass transformation in density classes is determined primarily by their location with respect to large-scale topography in ocean basins. Finally, in case of lee waves, the rate of the water-mass transformation is determined by the small, 1–10 km, scale topography that dominates the radiation of lee waves.

[17] The results described here represent a first attempt to estimate the leading order impact of internal wave-driven mixing on the global water-mass transformation in the deep ocean. It should be clear that these estimates are uncertain. The most significant sources of uncertainty are poorly constrained parameters in the mixing parameterization, which are spatially and temporally variable in the ocean, and the uncertainty of the energy conversion estimates due to poorly known rough topography and bottom flow characteristics. For instance, increasing the local dissipation efficiency, i.e. the fraction of wave energy that goes into irreversible mixing locally, from the 30% value used by *St. Laurent et al.* [2002] to 50%, a value suggested by idealized numerical simulations for lee waves [Nikurashin and Ferrari, 2010a; Nikurashin and Ferrari, 2010b], increases the maximum of the water-mass transformation driven by lee wave-driven mixing from 9 to 14 Sv (see supplementary material). A decrease to 10% as suggested by recent observations north of the Kerguelen Plateau [Waterman et al., 2012] would decrease the transformation from 9 to 3 Sv. New measurements and numerical simulations are needed to develop more robust parameterizations and constrain poorly known parameters. Our calculation provides a first quantitative description of the role of topographic internal wave-driven mixing. In particular, we believe that the result that lee wave-driven mixing is a leading order contributor to water-mass transformation in the deep ocean will stand the test of time.

[18] Currently, some ocean models include parameterizations for the mixing driven by tidal motions, while no parameterization exists for the mixing driven by lee waves. Ocean models are therefore likely to underestimate the water-mass transformation in the Southern Ocean, a region crucial for ocean carbon uptake. Furthermore, they may miss an important climate feedback, because the generation of lee waves by geostrophic motions is proportional to the surface wind stress which powers geostrophic variability in the Southern Ocean. Hence, the overturning circulation in the abyssal ocean may respond directly to changes in the Southern Hemisphere Westerlies through their modulation of lee wave-driven mixing.

[19] **Acknowledgments.** We would like to thank Jonas Nycander, Stephanie Waterman, Carl Wunsch, and an anonymous reviewer for their useful comments. This research was supported by the National Science Foundation under award OCE-1024198.

## References

- Garrett, C., and E. Kunze (2007), Internal Tide Generation in the Deep Ocean, *Ann. Rev. Fluid Mech.*, *39*, 57–87.
- Garrett, C., and L. St. Laurent (2002), Aspects of Deep Ocean Mixing, *J. Oceanogr.*, *58*, 11–24.
- Gouretski, V. V., and K. P. Koltermann (2004), WOCE Global Hydrographic Climatology. *A Technical Report 35*.
- Gregg, M. C. (1989), Scaling turbulent dissipation in the thermocline, *J. Geophys. Res.*, *94*, 9,686–9,698.
- Klocker, A., and T. J. McDougall (2010), The influence of the nonlinear equation of state on global estimates of diapycnal advection and diffusion, *J. Phys. Oceanogr.*, *40*, 1690–1709.
- Ledwell, J. R., et al. (1998), Mixing of a tracer in the pycnocline, *J. Geophys. Res.*, *103*, 21,499–21,529.
- Lumpkin, R., and K. Speer (2007), Global ocean meridional overturning, *J. Phys. Oceanogr.*, *37*, 2550–2562.
- Marshall, J., and K. Speer (2012), Closure of the meridional overturning circulation through Southern Ocean upwelling, *Nature Geosci.*, *5*, 171–180.
- Marshall, J., D. Jamous, and J. Nilsson (1999), Reconciling thermodynamic and dynamic methods of computation of water-mass transformation rates, *Deep-Sea Res. I*, *46*, 545–572.
- Munk, W. H. (1966), Abyssal recipes, *Deep-Sea Res.*, *13*, 707–730.
- Naveira Garabato, A., K. L. Polzin, B. A. King, K. J. Heywood, and M. Visbeck (2004), Widespread intense turbulent mixing in the Southern Ocean, *Science*, *303*, 210–213.
- Nikurashin, M., and R. Ferrari (2010a), Radiation and dissipation of internal waves generated by geostrophic flows impinging on small-scale topography: Theory, *J. Phys. Oceanogr.*, *40*, 1055–1074.
- Nikurashin, M., and R. Ferrari (2010b), Radiation and dissipation of internal waves generated by geostrophic flows impinging on small-scale topography: Application to the Southern Ocean, *J. Phys. Oceanogr.*, *40*, 2025–2042.
- Nikurashin, M., and R. Ferrari (2011), Global energy conversion rate from geostrophic flows into internal lee waves in the deep ocean, *Geophys. Res. Lett.*, *38*, L08610, doi:10.1029/2011GL046576.
- Nikurashin, M., and S. Legg (2011), A mechanism for local dissipation of internal tides generated at rough topography, *J. Phys. Oceanogr.*, *41*, 378–395.
- Nikurashin, M., and G. Vallis (2011), A theory of deep stratification and overturning circulation in the ocean, *J. Phys. Oceanogr.*, *41*, 485–502.
- Nurser, A. J. G., R. Marsh, and R. G. Williams (1999), Diagnosing Water Mass Formation from Air-Sea Fluxes and Surface Mixing, *J. Phys. Oceanogr.*, *29*, 1468–1487.
- Nycander, J. (2005), Generation of internal waves in the deep ocean by tides, *J. Geophys. Res.*, *110*, C10028, doi:10.1029/2004JC002487.
- Osborn, T. R. (1980), Estimates of the local rate of vertical diffusion from dissipation measurements, *J. Phys. Oceanogr.*, *10*, 83–89.
- Pedlosky, J. (1996), *Ocean Circulation Theory*, Springer-Verlag N.Y., 1998, 453p.
- Polzin, K. (2004), Idealized Solutions for the Energy Balance of the Finescale Internal Wave Field, *J. Phys. Oceanogr.*, *34*, 231–246.
- Polzin, K. L., J. M. Toole, J. R. Ledwell, and R. W. Schmitt (1997), Spatial variability of turbulent mixing in the abyssal ocean, *Science*, *276*, 93–96.
- Scott, R. B., J. A. Goff, A. C. Naveira Garabato, and A. J. G. Nurser (2011), Global rate and spectral characteristics of internal gravity wave generation by geostrophic flow over topography, *J. Geophys. Res.*, *116*, C09029, doi:10.1029/2011JC007005.
- Speer, K., and E. Tziperman (1992), Rates of Water Mass Formation in the North Atlantic Ocean, *J. Phys. Oceanogr.*, *22*, 93–104.
- St. Laurent, L. C., H. L. Simmons, and S. R. Jayne (2002), Estimating tidally driven mixing in the deep ocean, *Geophys. Res. Lett.*, *29*, 2106, doi:10.1029/2002GL015633.
- Stommel, H. (1958), The abyssal circulation, *Deep-Sea Res.*, *5*, 80–82.
- Walin, G. (1982), On the relation between sea-surface heat, ow and thermal circulation in the ocean, *Tellus*, *34*, 187–194.
- Waterman, S., A. C. Naveira Garabato, and K. L. Polzin (2012), Internal waves and turbulence in the Antarctic Circumpolar Current, *J. Phys. Oceanogr.*, doi:http://dx.doi.org/10.1175/JPO-D-11-0194.1.
- Wunsch, C. (1998), The work done by the wind on the oceanic general circulation, *J. Phys. Oceanogr.*, *28*, 2331–2339.